JOURNAL OF Applied Polymer SCIENCE

Investigating the Membrane Morphology of Water/Solvent/Nylon 6 Systems

Payman Sobhanipour, Mohammad Karimi
Department of Textile Engineering, Amirkabir University of Technology, Hafez Avenue, Tehran 15914, Iran
Correspondence to: M. Karimi (E-mail: mkarimi@aut.ac.ir)

ABSTRACT: In this study, nylon 6 membranes were prepared in a water coagulation bath with two types of solvents, $CaCl_2$–methanol (CaClMe) and formic acid (FA). The morphology of the membranes, which was controlled by the phase behavior of their solutions, were connected to the mechanism of demixing, including liquid–liquid and liquid-crystallization. Ternary phase diagrams showed that the CaClMe system coagulated significantly faster than the FA system. As observed by scanning electron microscopy, the CaClMe membrane had a porous, interconnected pore structure with macrovoids, whereas the FA membrane had a dense, spherulitic surface with a closed cell morphology. The high reaction surface of the CaClMe membrane with dye molecules provided outstanding dye rejection. Also, thermal analysis by differential scanning calorimetry showed that the slow coagulation of the FA system facilitated the formation of stable α-form crystals rather than a metastable γ-form structure. The results show that the phase-separation mechanism was switched from liquid–liquid to liquid-crystallization through a change in the solvent type from CaClMe to FA. © 2012 Wiley Periodicals, Inc. J. Appl. Polym. Sci. 000: 000–000, 2012

KEYWORDS: membranes; morphology; phase separation; polyamides

Received 17 January 2012; accepted 9 July 2012; published online
DOI: 10.1002/app.38328

INTRODUCTION

These days, porous polymeric membranes have widespread applications in many separation processes, including water and wastewater purification, desalination, and gas separation. Depending on the average pore size of the membrane top layer or active layer, membranes are categorized into microfiltration, ultrafiltration, nanofiltration, and reverse osmosis. The usual method of membrane fabrication is nonsolvent-induced phase separation. In the nonsolvent-induced phase separation process, a polymer solution with a concentration of about 10–30 wt % is immersed in a nonsolvent bath (typically water). Consequently, thermodynamic instability happens in the polymer solution and separates it into two phases, polymer-lean and liquid-crystallization. The polymer-rich phase forms the membrane matrix, which may solidify through different mechanisms, including gelation and/or crystallization. However, the polymer-lean phase, which is full of solvent and nonsolvent, makes the membrane pores. This kind of phase separation is called *liquid–liquid demixing* and is responsible for the appearance of porous structures. The shape, size, and distribution of the pores strongly depends on the exchange rate of solvent and nonsolvent, which is controlled by process variables, such as the coagulation bath composition and temperature and the composition of the polymer solution.[1–3]

Various materials have been used to prepare membranes, including inorganic ceramics and metals and organic polymers. In the large family of organic polymers, nylon is an engineering polymer with extensive applications in microfiltration and ultrafiltration processes because of its excellent mechanical, thermal, and chemical properties.[1,4–7] In nylon, the C═O group of a molecule is linked to N─H group of an adjacent molecule through a hydrogen bond. Therefore, the polymer can be crystallized during solidification. In such crystalline polymers, liquid–liquid and liquid-crystallization demixing are in competition with each other. According to the coagulation conditions, liquid–liquid and liquid-crystallization demixing may happen alone, simultaneously, or alternatively. Polyamide membrane structures formed through different coagulation conditions were studied by Shih et al.[8] A thin membrane skin and porous sublayer with a morphology of closed cells were attributed to the domination of liquid–liquid demixing. Moreover, when the membrane morphology contained crystal elements, such as sheaflike, sticklike, and/or spherulitic structures, crystallization was considered to be the main coagulation mechanism.

In some studies, the coagulation of nylon in water/formic acid (nonsolvent/solvent) system has been investigated, and various structures have been developed according to the coagulation conditions.[8–10] A number of researchers have tried to control

Table I. Characteristic Data of the Nonsolvent, Solvent, Polymer, and Dyes

Material	Molecular weight (g/mol)	Symbol	Density (g/cm^3)
Water	18.02	—	0.997
Formic acid	46.02	—	1.22
Methanol	32.04	—	0.79
$CaCl_2$	110.98	—	—
Nylon 6	34,000	—	—
Direct orange 34	299.29	DO34	—
Direct blue 86	780.17	DB86	—
Direct blue 158	1132.96	DB158	—

the morphology of nylon membranes by using different solvents. Tanaka[11,12] prepared nylon dopes in $CaCl_2$–methanol (CalClMe) and studied the coagulation in water. Zeni et al.[13] used chloride acid to dissolve nylon 66 and immersed the solution in water to prepare nylon 66 membranes. Shibata et al.[14] added different amounts of LiCl to FA/nylon 6 dopes to control the membrane morphology. They reported that for nylon 6 membranes prepared by changes in LiCl concentration, the value of water flux increased with increasing LiCl concentration in the range 6–8 wt %.

On the basis of what has been reported in the literature, metal halide salts, such as NaCl, $CaCl_2$, $MgCl_2$, CaF_2, and $GaCl_2$, prevent the crystallization of nylons when the polymer film is soaked in a salt aqueous solution or when the salts are mixed with a nylon melt.[15–17] Moreover, Vasanthan et al.[18] found that when a salted nylon 66 film (produced from the evaporation precipitation of $GaCl_2$–nitromethane/nylon 66 film) was regenerated (by salt extraction) through immersion in water, the resultant film showed a smaller degree of crystallization than a nylon 66 film precipitated from a FA/nylon 66 solution.

In this article, we show that salt prevents the growth of crystalline structures in nylons during precipitation. As mentioned previously, some researchers have applied acidic solvents and others have employed salt–alcohol to dissolve nylon for membrane preparation in separate studies. In this study, two solvents, FA and $CaCl_2$–methanol (CaClMe), were used to prepare nylon 6 membranes under the same coagulation conditions, and the phase behavior and mechanism of membrane formation were studied extensively.

EXPERIMENTAL

Materials

Nylon 6 from Tehran Fiber Co. (Tehran, Iran) was purchased in granule form. The nylon 6 molecular weight was determined to be 34,000 g/mol through intrinsic viscosity measurements (FA = 85 vol % at 28°C). Mark–Houwink parameters were $k = 0.023$ mL/g and $a = 0.82$.[19] Pure methanol, FA, and $CaCl_2$ (Merck, Germany) were used without further treatment. Distilled water was used wherever necessary. Three textile direct dyes, C. I. Direct Orange 34 (DO34), C. I. Direct Blue 86 (DB86), and C. I. Direct Blue 158 (DB158), were used to examine the membrane separation performance. The characteristics of the nonsolvent, solvent, polymer, and dyes are listed in Table I. Also, the molecular structures of the dyes are shown in Figure 1.

Membrane Preparation

A nylon 6 solution in CaClMe was prepared with 1.75 g of nylon 6, 2 g of $CaCl_2$, and 10 mL of methanol for a concentration of 15 wt % nylon 6. At first, $CaCl_2$ dissolved easily in methanol at 28°C. Then, nylon 6 granules were added to the CaClMe complex, heated, and refluxed at 65°C for several hours until the appearance of a clear and homogeneous solution. After the solution was cooled to 28°C, the solution was cast on a glass substrate with a manual membrane casting machine (Byk Gardner, Germany) with a thickness of 200 μm and was immediately immersed in a water bath at 28°C. To achieve complete salt extraction and decomplexation, the membrane was kept in the water bath for at least 24 h.

To dissolve nylon 6 in FA, appropriate amounts of nylon 6 granules were added to FA until a nylon 6 concentration of 15 wt % was easily obtained at 28°C. Again, the film thickness was 200 μm, and it was immediately immersed in water bath at 28°C. The nylon 6 membrane was kept in water for 24 h for completely solvent extraction.

Cloud-Point Experiments

The phase behavior of the ternary systems was studied through the cloud-point determination of the polymer solutions by titration with the nonsolvent at 28°C. Several dilute polymer solutions (1.5–12 wt %) were titrated with water with a micropipette. The addition of nonsolvent drops was stopped when the solution permanently became turbid. Then, the final mass fraction of the component was calculated and plotted in a ternary phase diagram.

Membrane Characterization

To evaluate the membrane performance, the water permeability and dye rejection were measured by a laboratory dead-end module. The scheme of this module is shown in Figure 2. The driving force was provided by a nitrogen gas push. A magnet close to the membrane surface stirred the dye solution to

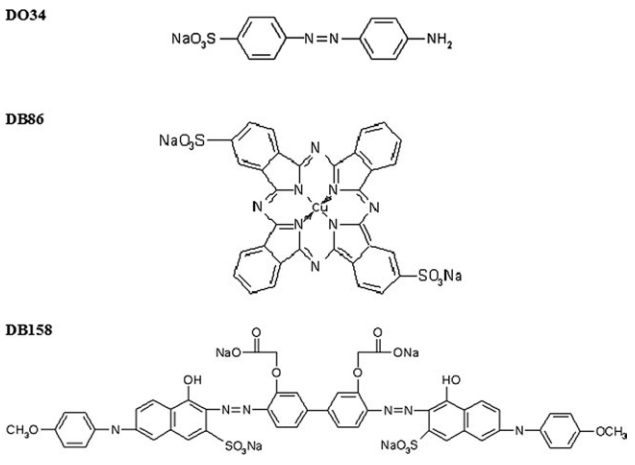

Figure 1. Chemical structure of the dyes used for the dye-rejection measurements.

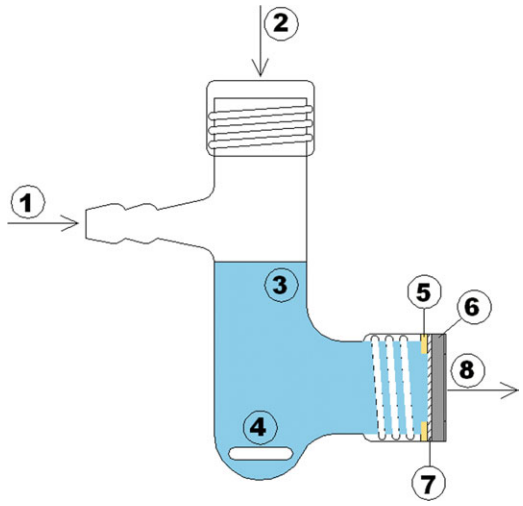

Figure 2. Scheme of the laboratory dead-end module: (1) nitrogen inlet, (2) feed inlet, (3) feed solution, (4) magnet, (5) silicon sealing ring, (6) membrane support, (7) membrane, and (8) permeate outlet. [Color figure can be viewed in the online issue, which is available at wileyonlinelibrary.com.]

prevent membrane fouling. During both the water permeability and dye rejection tests, the transmembrane pressure (TMP), effective membrane area, and working temperature were 1×10^5 Pa, 1.54×10^{-4} m^2, and 28°C, respectively.

To obtain the water permeability of the membrane, the permeate water was periodically collected and weighed. Then, the permeate water volume as a product of the time and effective membrane area was plotted. Consequently, the slope of the best fitting line gave the membrane water permeability at the working TMP.

Aqueous solutions of the three direct dyes (DO34, DB86, and DB158) were prepared in water and fed to the membrane module. The initial concentration of each of the dyes was 200 ppm. Equation (1) was used for the determination of dye rejection:[1,20,21]

$$R = \left(1 - \frac{C_p}{C_f}\right) \times 100 \quad (1)$$

where R is the percentage rejection of the dye and C_p and C_f are the concentrations of the permeate and feed solutions, respectively. The concentration of the dye in permeate was measured with a Cary 100 UV–vis spectrophotometer at the wavelength of maximum absorbance (λ_{max}).

Morphological Investigation

To observe the morphologies of the membrane skin and cross section, scanning electron microscopy (SEM) observations were done with a Philips XL30 apparatus. Dry samples were fractured in liquid nitrogen and then coated with a thin layer of gold.

Thermal Analysis

The melting temperature of nylon 6 membranes was obtained with a differential scanning calorimetry (DSC) instrument from TA Instruments (model 2010). About 5 mg of each sample was put into a nonhermitic DSC pan and heated at rate of 10°C/min under a nitrogen atmosphere. Temperature calibration was done with indium. To determine the degree of crystallinity (X_{cr}), eq. (2) was used:[22]

$$X_{cr} = \frac{\Delta H}{\Delta H^0} \times 100 \quad (2)$$

where $\Delta H^0 = 26.0$ kJ/mol is the heat of fusion for a 100% crystalline nylon 6 and ΔH is the heat of fusion for the sample and was obtained through the melting peak area.[23]

RESULTS AND DISCUSSION

Water Permeability

From this point on, the water/CaClMe/nylon 6 and water/FA/nylon 6 systems are abbreviated by the CaClMe and FA systems, respectively. Also, the resulting membranes from the CaClMe and FA systems are called the CaClMe and FA membranes, respectively. The water permeability results for the CaClMe membrane showed an average value of 19.55 L/m^2/h at a TPM of 1 bar. However, at this TMP, the water permeability of the FA membrane was zero. In fact, the FA membrane surface was so dense that a driving pressure of 1 bar was not enough to make it permeable.

Dye Rejection

The separation performance of the CaClMe membrane was examined by the three textile direct dyes. Figure 3 presents the rejections of DO34, DB86, and DB158 at a TMP of 1 bar and operation temperature of 28°C. The result shows that dye rejection increased with the molecular weight of dye. This meant that when the molecular weight of the dye increased, van der Walls attraction forces significantly appeared, and hence, it was more possible that the dyes with such rigid structures were captured in the membrane pores. Direct dyes are widely used to dye cotton textile products. These dyes have auxochrome groups, such as carboxyl, sulfonic, and hydroxyl groups, that make them soluble in water. Therefore, the rejection values of about 74% for DO34, 84% for DB86, and 100% for DB158 demonstrated that sieving was certainly not the rejection

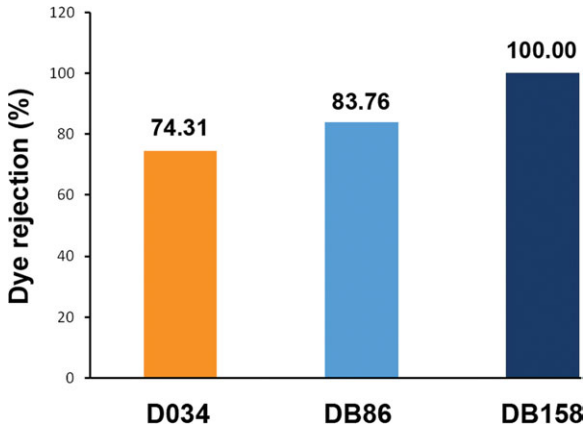

Figure 3. Dye rejection of the direct dyes: DO34, DB86, and DB158 at a TMP of 1 bar by a CaClMe membrane. [Color figure can be viewed in the online issue, which is available at wileyonlinelibrary.com.]

Applied Polymer SCIENCE

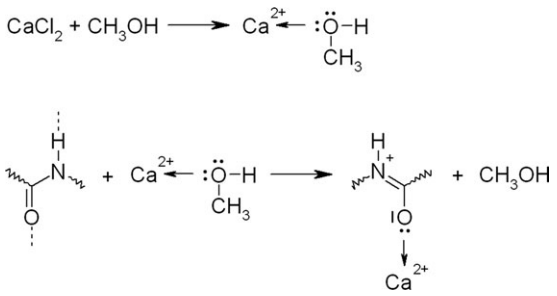

Figure 4. Dissolving mechanism of nylon 6 in CaClMe.[25]

mechanism here, especially when the driving pressure was only 1 bar. Deeper studies by SEM will probably clarify this question.

Phase Behavior of the Water/Solvent/Nylon 6 Systems

Before any discussion about the phase diagrams of the water/solvent/nylon 6 systems, we focus on the nature of the solvents and the state of the polymer in the solution. FA is the simplest carboxylic acid; it is polar and easily dissolves nylon 6 at 28°C. However, this solvent is distasteful for the operator and partially degrades nylon, especially at high temperatures.[24] The application of a CaClMe complex as a solvent for nylons was introduced by Schupp[25] for the first time in 1940. Nylon 6 is not solvable in methanol. However, by stirring and heating it in the complex of CaClMe, one can gradually dissolve nylon 6 granules. Only a few researchers have studied the dissolving mechanism of nylons in salt–alcohol complexes.[24,26] The dissolving mechanism of nylon 6 in CaClMe, as proposed by Benhui,[24] is demonstrated in Figure 4.

In a ternary system of nonsolvent, solvent, and polymer, there are many potential mass transfer paths during phase separation because of the different process conditions that make various membrane structures.[27] The phase behavior of a ternary system is studied through the phase diagram, which gives the compositions of the nonsolvent, solvent, and polymer at a certain pressure and temperature. A typical phase diagram is composed of a binodal or liquid–liquid phase separation boundary, which divides the phase diagram into two regions, homogeneous (one phase) and heterogeneous (two phases). The area of the one-phase region shows how the system is miscible and thermodynamically stable. In other words, the larger the miscibility region is, the more stable system and better the interaction between the polymer and solvent will be.

The phase diagrams of the CaClMe and FA systems are given in Figure 5. It was clear that miscibility area for the FA system was larger than that of the CaClMe system. This means there was better interaction in FA/nylon 6 than in CaClMe/nylon 6. To put it another way, the coagulation capacity for the FA system was greater than that of the CaClMe system, or the CaClMe system was coagulated by less nonsolvent. This condition caused instantaneous phase separation for the CaClMe system. Therefore, fast precipitation probably made macrovoids and/or a porous structure, which were explained by Kim et al.[28]

Morphology Study

SEM images of the CaClMe and FA membranes are given in Figures 6(a–e) and 7(a–c). The figures show that the CaClMe membrane had ultrathin skin with a thickness of about a few hundred nanometers. Cellular pores, with sizes between 1 and 1.5 μm, formed exactly below the membrane top layer. Moreover, a vast portion of the membrane contained macrovoids that had been significantly distributed in the lower part of the membrane cross section. They showed apparent deviation from the typical fingerlike shape and were different in size and form. Generally, macrovoid formation is an undesirable phenomenon because it decreases the membrane mechanical strength. There are a lot of different theories in the literatures that try to explain the formation of macrovoids. As a general idea, macrovoid formation is facilitated in systems with rapid coagulation.[1,28] It was also confirmed by the small miscibility area in the CaClMe system (see Figure 5).

For more precise analysis of macrovoid formation, the theories of Strathmann[29,30] and Smolders et al.[29–31] are employed. Strathmann believed that macrovoids appear as the result of the rapid diffusion of nonsolvent at loose spots on the membrane skin. This situation makes a similar morphology for the membrane skin and macrovoid wall; that is, there is the same coagulant or coagulation conditions for the membrane skin and macrovoid wall. The porous surface of the CaClMe membrane, with pores of about 10–500 nm [Figure 6(c, d)], and a macrovoid wall with an average pore size of 1 μm [Figure 6(e)] confirmed Strathmann's approach. However, it was still questionable as to why the pore size of the macrovoid wall was larger than that of the membrane surface. It is clear that during precipitation, the solvents, including $CaCl_2$ and methanol, were rejected from the membrane matrix into the voids. Therefore, the combination of nonsolvent and solvent made a soft local bath, as Smolders mentioned. This soft bath postponed phase separation and let the polymer-poor phases grow. We better explain the Strathmann and Smolders hypotheses schematically in Figure 8.

The distinguishing feature of the CaClMe membrane is its porous surface. In fact, at the interface of polymer solution and

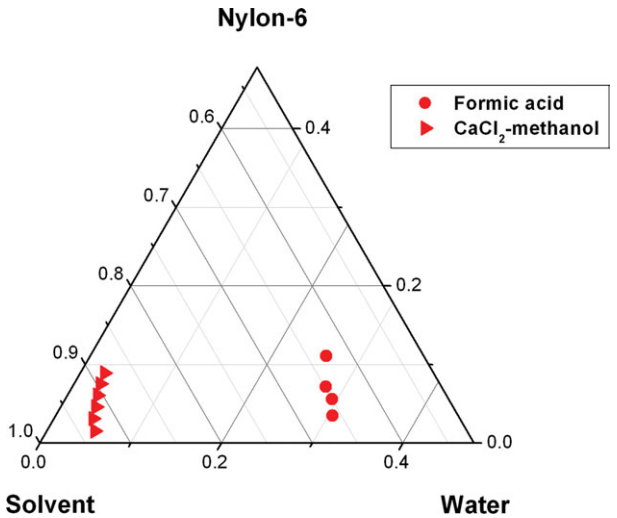

Figure 5. Phase diagram of the (▶) CaClMe system and (●) FA system. [Color figure can be viewed in the online issue, which is available at wileyonlinelibrary.com.]

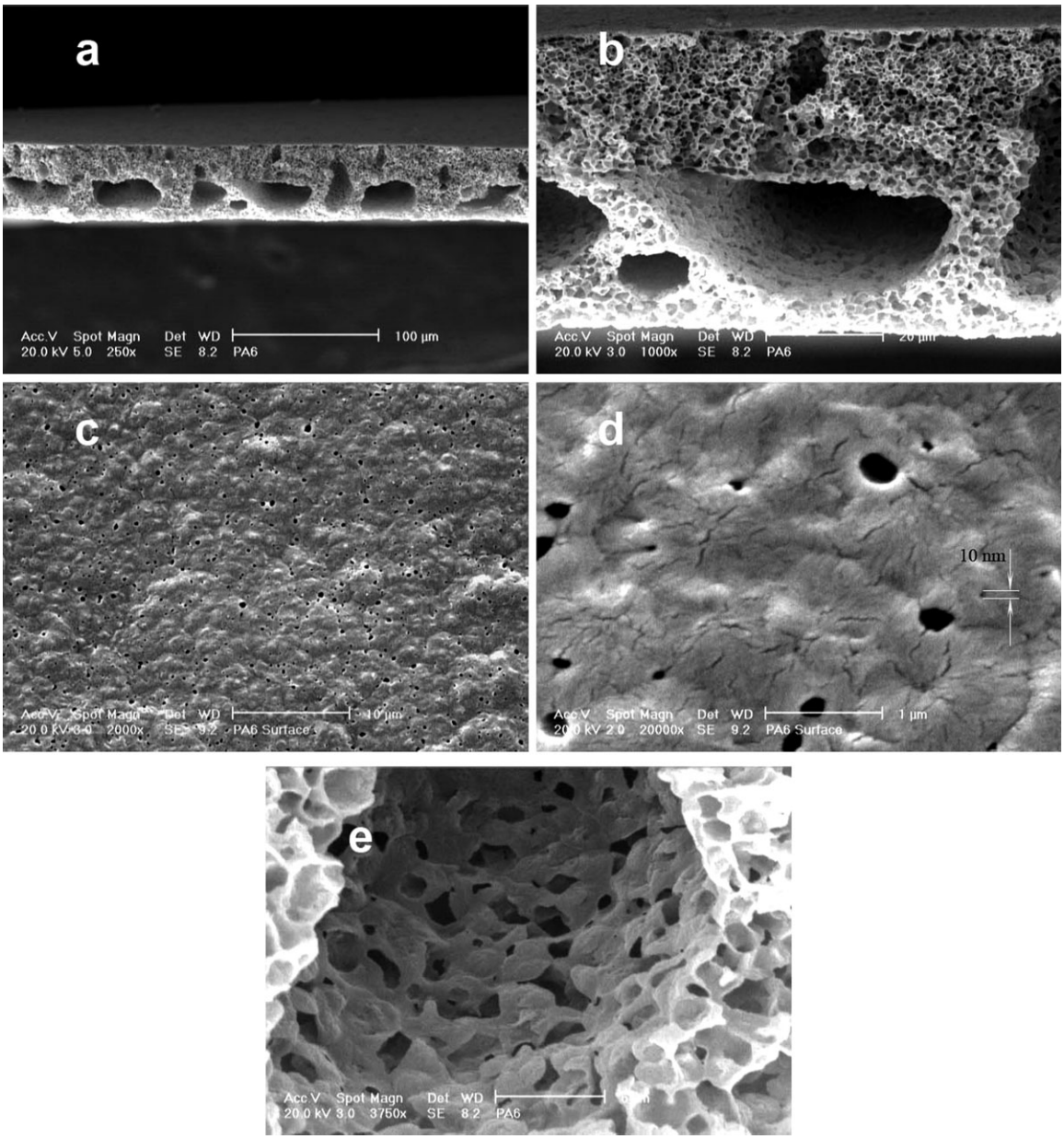

Figure 6. SEM image of the CaClMe membrane: (a) cross section (magnification = 250×), (b) cross section (magnification = 1000×), (c) surface (magnification = 2000×), (d) surface (magnification = 20,000×), and (e) macrovoid wall (magnification = 3750×).

the coagulation bath, although the coagulation rate was very high, nuclei of the polymer-lean phase appeared and grew. To put it another way, the combination of imperfect spherulitic crystals and pores on the membrane surface [Figure 6(c, d)] demonstrated that there was intensive competition between the liquid–liquid and liquid-crystallization demixing. In fact, nylon 6 is naturally a crystalline polymer, which tends to be crystallized during coagulation. On the other hand, the existence of salt in the vicinity of the polymer molecules prevents the growth of crystalline structures, as discussed before. This situation is well demonstrated in Figure 6(d), where faded spherulites with many pores and cracks on the membrane surface are shown.

The FA membrane had completely different structure. It had a thick skin, with a thickness of about 2–4 μm. Also, the membrane surface was full of polygonal spherulites with clear boundaries. Such observations were reported by Lin et al.[9] for nylon 6,6 precipitated from a water/FA/nylon 6,6 system. Also, there was a uniform distribution of pores with a size of about 3 μm in the membrane sublayer, and no macrovoid-like CaClMe membrane was observed. Because the FA system had a larger miscibility region than the CaClMe system and consequently slower coagulation, crystalline structures could grow and develop.

Next, the water permeability, dye rejection, and SEM data were analyzed all together. The data showed that the CaClMe

Applied Polymer SCIENCE

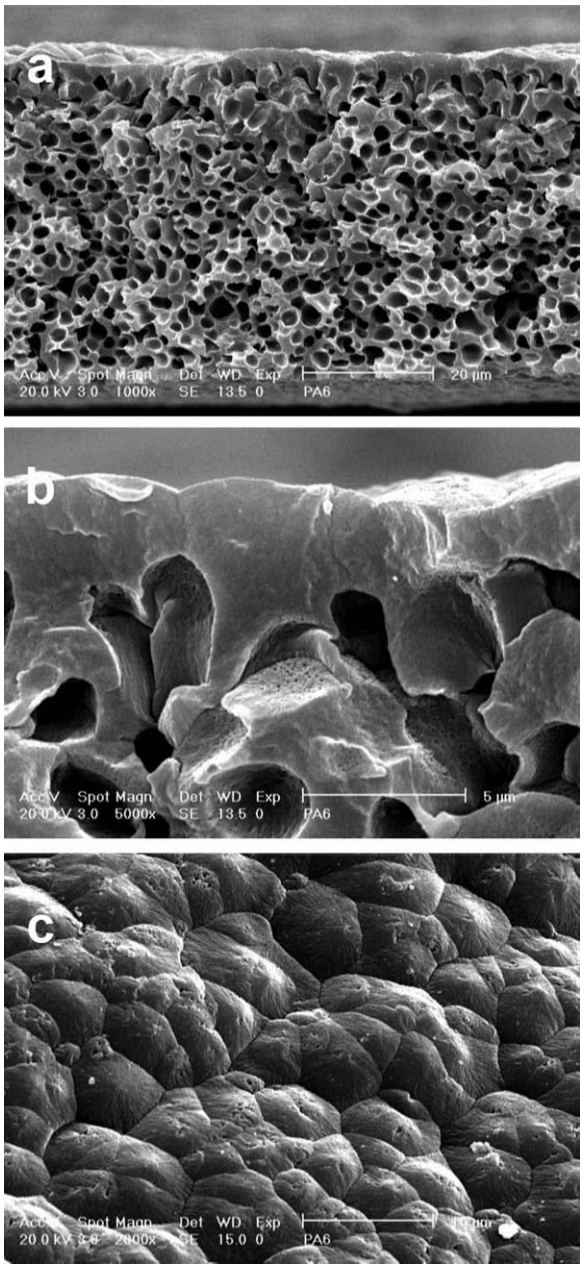

Figure 7. SEM image of the FA membrane: (a) cross section (magnification = 1000×), (b) cross section (magnification = 5000×), and (c) surface (magnification = 2000×).

membrane was water permeable at a TMP of 1 bar because of its porous surface and interconnected sublayer pores. Also, it was easy to determine that a driving pressure of 1 bar was not enough for water to overcome the dense crystalline surface of the FA membrane and penetrate into it that resulted in zero water permeability at this TMP. Moreover, it is understood that the CaClMe membrane provided a high interaction surface with the dye molecules because of its porous and permeable structure, which provided such a high dye rejection for those water-soluble particles. To put it another way, the nylon membrane was stained by the dye molecules. Consequently, we determined

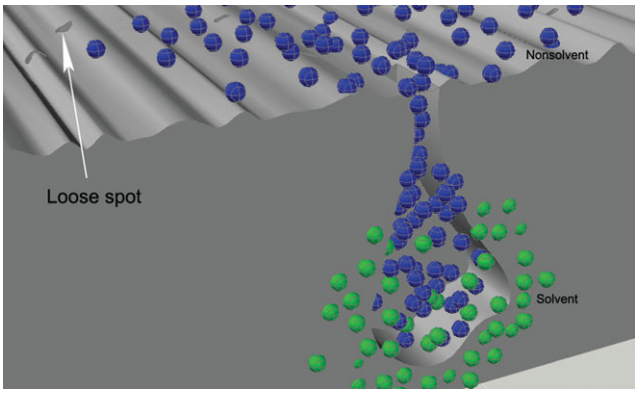

Figure 8. Schematic representation of the macrovoid formation by Strathmann and Smolders. [Color figure can be viewed in the online issue, which is available at wileyonlinelibrary.com.]

from the data that the charge interaction was the main rejection mechanism in the CaClMe membrane.

Thermal Analysis

Figure 9 shows the DSC thermographs of the nylon 6 granules, the CaClMe membrane, and the FA membrane. Also, the melting temperatures and degrees of crystallization are presented in Table II. The thermal behavior of the membranes was significantly different that signified distinct structural properties. The DSC curve of the nylon 6 granules had a single sharp peak at 221°C. However, the CaClMe membrane showed two shoulders at 204 and 217°C and a main peak at 220°C, whereas the FA membrane had a shoulder at 207°C and a main peak at 218°C. There were two crystalline structures, α form and γ form, in nylon 6. The molecules in α form were fully extended, with a planar zigzag chain conformation; this is a thermodynamically stable structure and well formed under slow crystallization, whereas the γ form is a helical and metastable structure, which is formed by rapid crystallization.[32] As discussed before, the CaClMe membrane precipitated faster than the FA membrane.

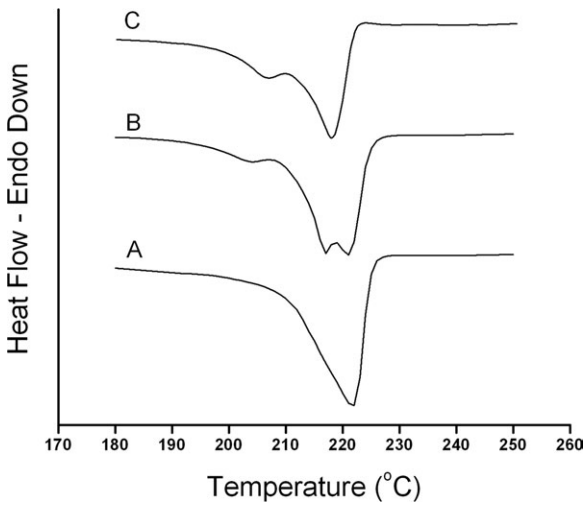

Figure 9. DSC thermograph of the (A) nylon 6 granule, (B) CaClMe membrane, and (C) FA membrane.

Table II. Melting Point and Degree of Crystallization Values for the CaClMe Membrane, FA Membrane, and Nylon 6 Granule

	Melting point (°C)		Degree of crystallization (%)
	Shoulders	Main peak	
CaClMe membrane	204 and 217	220	33
FA membrane	207	218	37
Nylon 6 granules	—	221	46

Therefore, the α-form crystal was favored in the FA membrane compared to the CaClMe membrane that resulted in a greater crystallization degree and less shoulder or more perfect crystals than the CaClMe membrane.

CONCLUSIONS

In this study, nylon 6 membranes were prepared by the phase inversion of CaClMe/nylon 6 and FA/nylon 6 solutions in water. The findings by ternary phase diagrams showed that the water/CaClMe/nylon 6 system had a smaller miscibility area than the water/FA/nylon 6 and coagulated faster. This situation created a very porous membrane with macrovoids in its structure. In other words, liquid–liquid demixing was dominant in the water/CaClMe/nylon 6 system. On the other hand, because the coagulation rate of the FA/nylon 6 solution in water was slower, crystalline structures, including spherulites, were formed. Our nylon 6 membrane, prepared by the CaClMe solvent, showed a water permeability of 19.55 L/m^2/h at a TPM of 1 bar because of its porous surface and sublayer, whereas the water/FA/nylon 6 membrane was not permeable at that TMP because of its dense and thick crystalline surface. Moreover, our porous water/CaClMe/nylon 6 membrane provided a wide interaction surface with the dye molecules and could reject them effectively.

The major conclusion that was drawn with what was investigated in this research was that the coagulation mechanism was changed from liquid–liquid demixing to liquid-crystallization by a change of the solvent from CaClMe to FA.

REFERENCES

1. Mulder, M. Basic Principles of Membrane Technology; Elsevier: Amsterdam, **1991**.
2. Karimi, M.; Albrecht, W.; Heuchel, M.; Kish, M. H.; Frahn, J.; Weigel, T.; Hofmann, D.; Modarress, H.; Lendlein, A. *J. Membr. Sci.* **2005**, *265*, 1.
3. Van de Witte, P.; Dijkstra, P. J.; Van den Berg, J. W. A.; Feijen, J. *J. Membr. Sci.* **1996**, *117*, 1.
4. Zhang, Z. B.; Zhu, X. L.; Xu, F. J.; Neoh, K. G.; Kang, E. T. *J. Membr. Sci.* **2009**, *342*, 300.
5. Xia, B.; Zhang, G.; Zhang, F. *J. Membr. Sci.* **2003**, *226*, 9.
6. Singh, R. Hybrid Membrane Systems for Water Purification: Technology, Systems Design and Operation; Elsevier: Great Britian, **2006**.
7. Vasileva, N.; Godjevargova, T. *J. Membr. Sci.* **2004**, *239*, 157.
8. Shih, C.-H.; Gryte, C. C.; Cheng, L.-P. *J. Appl. Polym. Sci.* **2005**, *96*, 944.
9. Lin, D.-J.; Chang, C.-L.; Lee, C.-K.; Cheng, L.-P. *Eur. Polym. J.* **2006**, *42*, 356.
10. Young, T.-H.; Lin, D.-J.; Gau, J.-J.; Chuang, W.-Y.; Cheng, L.-P. *Polymer* **1996**, *40*, 5011.
11. Tanaka, N. *Polymer* **1995**, *36*, 2597.
12. Tanaka, N. *Polymer* **1996**, *37*, 2201.
13. Zeni, M.; Riveros, R.; De Souza, J. F.; Mello, K.; Meireles, C.; Filho, G. R. *Desalination* **2008**, *221*, 294.
14. Shibata, M.; Kobayashi, T.; Fujii, N. *J. Appl. Polym. Sci.* **2000**, *75*, 1546.
15. More, A. P.; Donald, A. M. *Polymer* **1992**, *33*, 4081.
16. Tanaka, N.; Fukushima, T. *Thermochim. Acta.* **2003**, *396*, 79.
17. Muellerleile, J. T.; Freeman, J. J.; Middleton, J. C. *J. Appl. Polym. Sci.* **1998**, *69*, 1675.
18. Vasanthan, N.; Kotek, R.; Jung, D.-W.; Shin, D.; Tonelli, A. E.; Salem, D. R. *Polymer* **2004**, *45*, 4077.
19. Mark, J. E. Polymer Data Handbook; Oxford University Press: **1999**.
20. Mo, J. H.; Lee, Y. H.; Kim, J.; Jeong, J. Y.; Jegal, J. *Dyes Pigments* **2008**, *76*, 429.
21. Azari, S.; Karimi, M.; Kish, M. H. *Ind. Eng. Chem. Res.* **2010**, *49*, 2442.
22. Li, X.; Wang, Y.; Lu, X.; Xiao, C. *J. Membr. Sci.* **2008**, *320*, 477.
23. Wunderlich, B. Thermal Analysis of Polymeric Materials; Springer: **2005**.
24. Benhui, S. *Chin. J. Polym. Sci.* **1994**, *12*, 57.
25. Schupp, D. E. (to DuPont). U.S.Pat. 2,359,877 (**1940**).
26. Nakajima, A.; Tanaami, K. *Polym. J.* **1973**, *5*, 248.
27. Stropnic, C.; Musil, V.; Brumen, M. *Polymer* **2000**, *41*, 9227.
28. Kim, Y. D.; Kim, J. Y.; Lee, H. K.; Kim, S. C. *J. Appl. Polym. Sci.* **1999**, *74*, 2124.
29. Strathmann, H. *Am. Chem. Soc. Symp. Ser.* **1985**, *269*, 165.
30. Strathmann, H.; Koch, K. *Desalination* **1997**, *21*, 241.
31. Smolders, C. A.; Reuvers, A. J.; Boom, R. M.; Wienk, I. M. *J. Membr. Sci.* **1992**, *73*, 259.
32. Cho, D.; Zhmayev, E.; Joo, Y. L. *Polymer* **2011**, *52*, 4600.